Tip-on-fiber Electro-optic Probe for Near-field Measurement

Hiroyoshi Togo[†], Naofumi Shimizu, and Tadao Nagatsuma

Abstract

We have developed a tip-on-fiber electro-optic (EO) probe for electric field measurement. It can detect longitudinal and transverse fields depending on how the EO crystal planes are configured. Because the tip of the EO probe consists of a 1-mm^3 cubic EO crystal and contains no metallic components, it causes very little disturbance of the electric field during measurement. The fabricated EO probe has flat sensitivity from 1.95 to 20 GHz and directivity with cross-axis sensitivity isolation greater than 45 dB. A comparison of the measured and calculated near fields of a dipole showed negligible static or inductive coupling between the EO probe and the dipole. We demonstrated the potential of the EO probe in electric field intensity and phase measurements using a tissue-equivalent phantom.

1. Introduction

The antenna is one of the most important parts of systems that use microwave and millimeter-wave electromagnetic fields for wireless communication, sensing, or processing because its characteristics greatly influence system performance. Therefore, for wireless system development it is very important to establish a method that enables us to precisely char- acterize antennas. Antenna characterization is per- formed in various ranges under various circum- stances (**Table 1**). In far-field ranges, the characteris- tics are directly obtained from measured data. How- ever, these ranges require a huge measurement envi- ronment in order to avoid electric field disturbances due to reflections from objects other than the antenna under test (AUT). In near-field ranges, measurements are performed in an anechoic chamber and the data is

Table 1.   Characteristics of antenna-measurement methods.

Range	Site	Description	Advantages	Disadvantages
Far-field	Open	Source and test antenna are placed on tower, building, hill, etc. Either the source or test antenna is elevated.	Low cost	Requires real estate May require towers Subject to outdoor weather
	Inside anechoic chamber	Room is lined with absorber material to suppress reflections.	Indoors	Absorber and large room are costly.
Near-field	Inside anechoic chamber	Magnitude and phase of the near field of the test antenna are sampled and the far field is computed.	Very small space	Accurate probe positioning is required. Accurate amplitude and phase are required. Measurements are time-consuming and computer-intensive

† NTT Microsystem Integration Laboratories
  Atsugi-shi, 243-0198 Japan
  E-mail: togo@aecl.ntt.co.jp
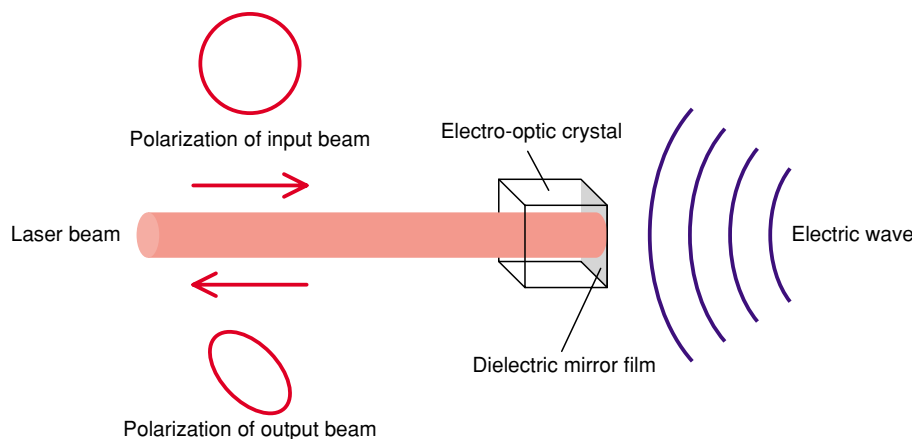
Ubiquitous Applications

Fig. 1.   Principle of electric field measurement using EO crystal.

converted to far-field characteristics by numerical calculation.

In a near-field measurement, it is common to scan a metallic probe such as a horn antenna, a dipole antenna, or the edge of a waveguide around the AUT [1]-[3]. However, errors are caused by the electric field disturbances due to reflection from the probe and by electrical coupling between the probe and AUT. To solve this problem, an electro-optic (EO) probe was proposed as an alternative [4], [5]. In the probes described in [4], [5], a Mach-Zehnder interferometer is integrated on a LiNbO3 substrate and a miniature dipole antenna fabricated on a waveguide. The electric field detected at the dipole antenna is converted to an optical-intensity-modulated signal and transmitted to a receiver through an optical fiber. Therefore, waveguide-based EO probes are less invasive than the conventional metallic probes. However, at high frequencies, the invasiveness of the dipole antenna may not be negligible. To reduce it, we have developed a pen-shaped EO probe based on a bulk EO crystal [6]. The bulk EO crystal was fixed on the tip of the pen-shaped cylinder housing the optical components. This probe had flat sensitivity from several megahertz to several hundred gigahertz. However, invasiveness due to reflection from the cylinder and the optical components inside it was still a problem for more accurate measurement. To solve this problem, we recently developed a tip-on-fiber EO probe where the EO crystal is connected to the optical components with an optical fiber.

The next section describes the principle and system configuration of the developed EO probe. Section 3 discusses the invasiveness of the EO probe in an electric field and describes basic characteristics, such as the dynamic range, frequency response, and directiv-

ity. Section 4 describes a near-field measurement around a dipole antenna in free space as one application of the probe and an electric field measurement in a tissue-equivalent phantom (TEP)[*] as another application.

2.   System configuration

2.1   EO probe

An EO crystal changes its birefringence when an electric field is applied to it. This is called the Pockels effect and our measurement system uses this effect. The principle of electric-field measurement with an EO crystal is shown in **Fig. 1**. When there is no electric field, a laser beam input to an EO crystal is reflected back by a dielectric mirror with its polarization unchanged. When there is an electric field, the index tensor changes. As a result, the laser beam is reflected back with a change in polarization. After the polarization change has been converted to a change in optical intensity by a polarizer, we obtain a signal that is proportional to the electric field intensity. A side view of the EO probe tip with a CdTe crystal is shown in **Fig. 2**. Besides the EO crystal, the tip contains a dielectric mirror, a collimating lens, and a glass ferrule. The diameter of the laser beam is 0.4 mm. The EO crystal is a 1-mm^3 cube, so its cross-section is smaller than that of the dipole antenna in a waveguide-based EO probe [4], [5]. This small EO probe tip reduces the invasiveness and the space needed for measurement. The whole EO probe is shown in **Fig.**

---

*   The tissue-equivalent phantom has been developed to evaluate the interaction between the human body and an electromagnetic field. It has electrical constants adjusted to match those of the human body.
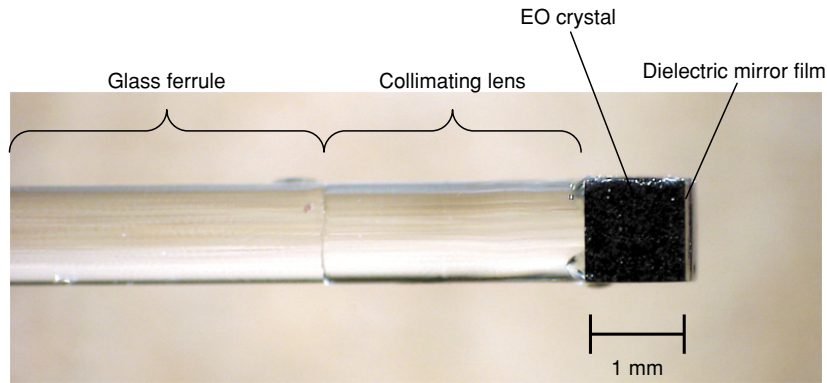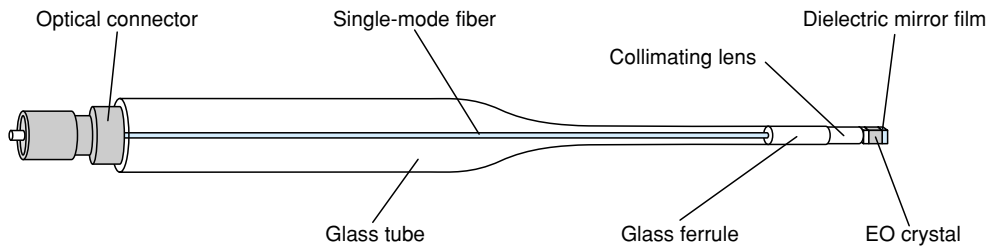
Fig. 2. Tip of EO probe.

Fig. 3. EO probe.

3. The EO probe tip and an optical fiber connector are fixed at opposite ends of a glass tube 5 mm in diameter and 300 mm long and connected by a single mode fiber. This EO probe is directly attached to a polarization control module by the fiber connector.

The EO probe uses a CdTe crystal, which is an optically isotropic crystal with a zinc-blende crystal lattice. We made a longitudinal field probe to detect an electric field parallel to the propagation direction of a laser beam (**Fig. 4(a)**) and a transverse field probe to detect an electric field orthogonal to the propagation direction (**Fig. 4(b)**). Both probes exhibit the same sensitivity because the crystal has a cubic structure.

2.2 Electric field measurement system

A block diagram of an electric field measurement system using the EO probe is shown in **Fig. 5**. The system

(a) Longitudinal field probe
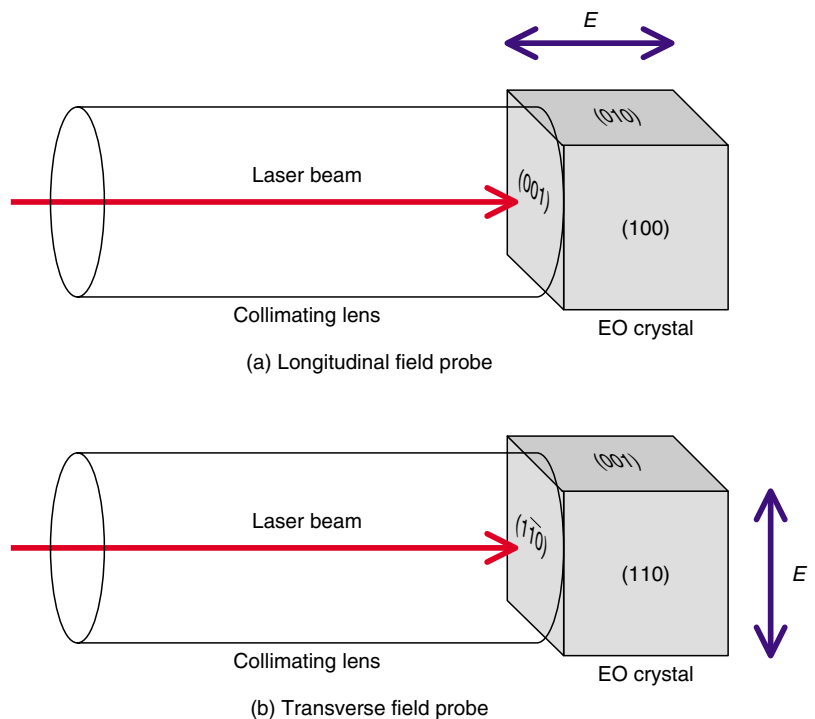

(b) Transverse field probe

Fig. 4. Relationship between crystal plane directions and detectable direction of electric field.
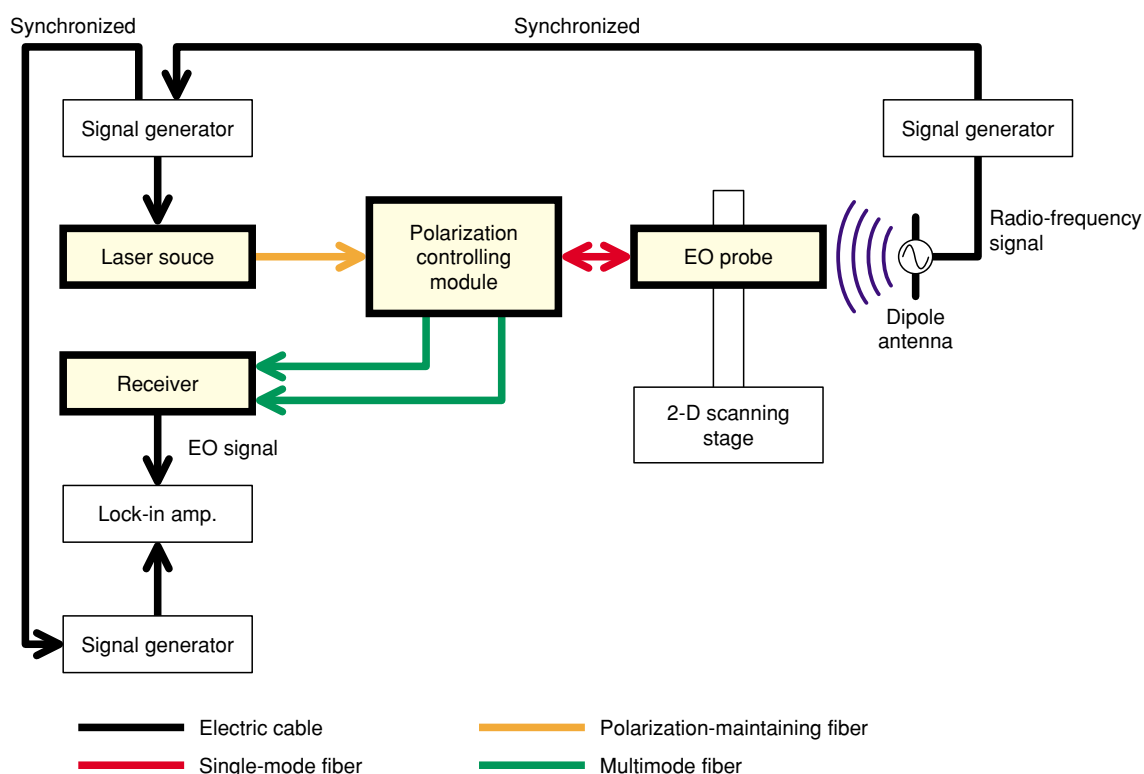
Fig. 5. Block diagram of electric field measurement system using EO probe.

comprises a laser source, polarization control module, EO probe, receiver, two-dimensional (2D) scanning stage, lock-in amplifier or spectrum analyzer, and three signal generators. The laser source emits a linearly polarized light, which is sent to the polarization control module via a polarization-maintaining fiber and then delivered to the EO probe. The delivered light is reflected by the dielectric mirror inside the probe and returned to the receiver after it has been spilt into two lights with orthogonal polarizations. The received lights are converted to electrical signals by balanced photodetectors and a differential amplifier. The signal intensity is proportional to the change in polarization. The lock-in amplifier measures the intensity of the obtained electrical signal, which coincides with that of the applied electric field.

3. Basic properties

3.1 Electric field around the EO probe

We calculated the electric field intensity around the EO probe in free space using the finite integration
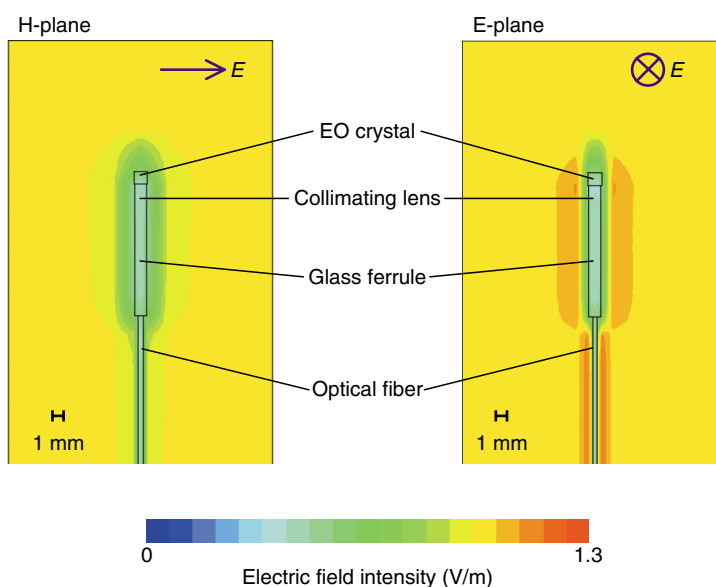

Fig. 6. Calculated electric field around EO probe in tissue-equivalent phantom.

method. The E- and H-planes of the electric field (each 20 mm × 30 mm) are shown in **Fig. 6**. The calculated region was a rectangular parallelepiped 50 mm high and 200 mm long. The electromagnetic

wave was a plane wave oscillated at 1.95 GHz. Periodic boundary conditions were assigned on planes orthogonal to the propagation direction and a perfectly matched layer was assigned on the output plane. The degree of intensity is represented by color gradation. The figure shows that there was no disturbance in the region more than 2 mm away from the EO probe.

3.2 Sensitivity

The relationship between the input power to the dipole antenna and the EO signal intensity measured with the longitudinal field probe is shown in **Fig. 7**. The sensitivity of the EO probe was measured using an electric field radiated in free space from a half-wavelength dipole antenna (Anritsu MA5612B4) under the conditions described below. The dipole antenna, EO probe, polarization control module, and 2D scanning stage were set inside an RF (radio frequency) shielded box with dimensions of $900 \times 900 \times 900$ mm^3 and all other instruments were set outside. The return loss of the box's inner walls was more than 40 dB. The center of the EO crystal was kept at a distance of 5 mm from the feeding point of the dipole antenna, while the signal generator input a sinusoidal signal with a frequency of 2.45 GHz to the dipole antenna. The dynamic range was over 45 dB. The minimum detectable electric field intensity defined by the noise floor was less than 0.6 V/m. The transverse field probe was similarly measured and it showed the same sensitivity.

3.3 Directivity

The directivities of the longitudinal and transverse field probes are shown in **Figs. 8** and **9**, respectively. In this measurement, the tip of the EO probe was positioned 5 mm from the feeding point of a 2.45-GHz-band dipole antenna driven by a sinusoidal signal. For the longitudinal field probe, the dipole antenna was rotated on planes perpendicular to the (100) or (010) planes of the EO crystal. For the transverse field probe, the dipole antenna was rotated on a plane parallel to the (1$\bar{1}$0) plane. In Fig. 8, closed and open circles represent the directivities on the (100) and (010) planes, respectively, and the solid line
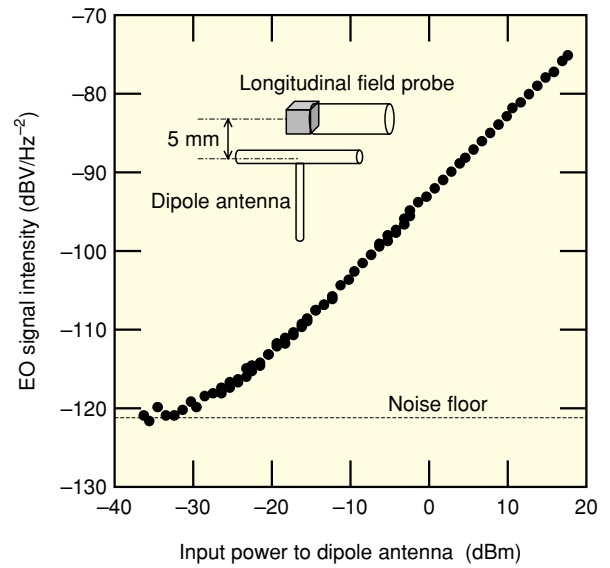

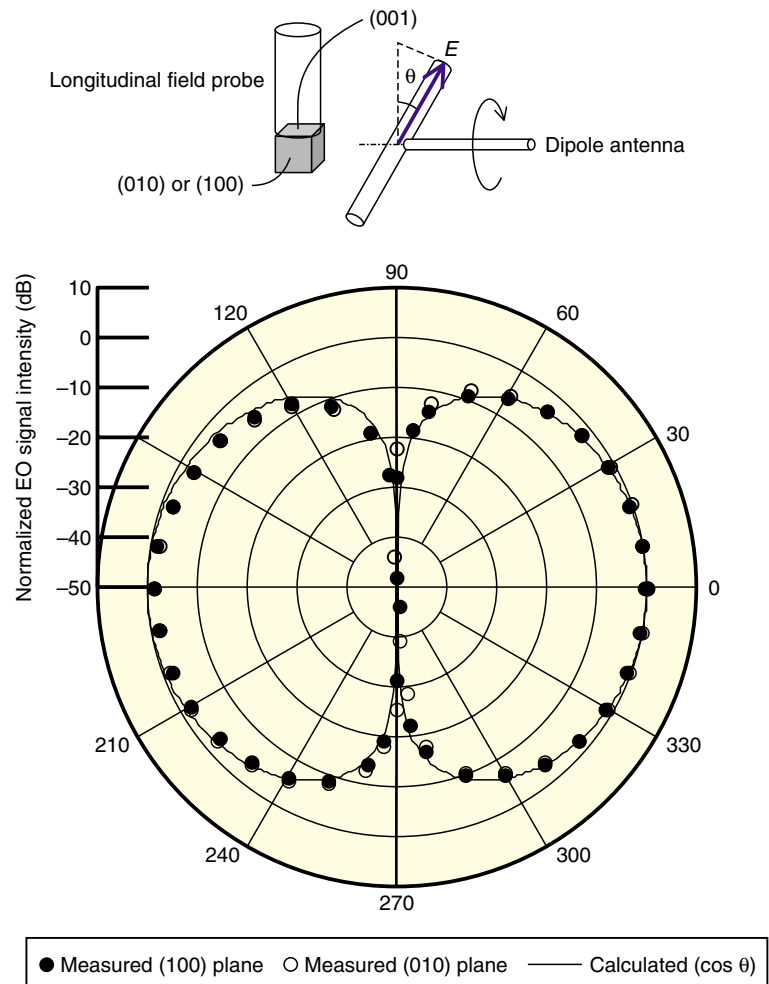Fig. 7. Dependence of sensitivitiy on input power to dipole antenna.

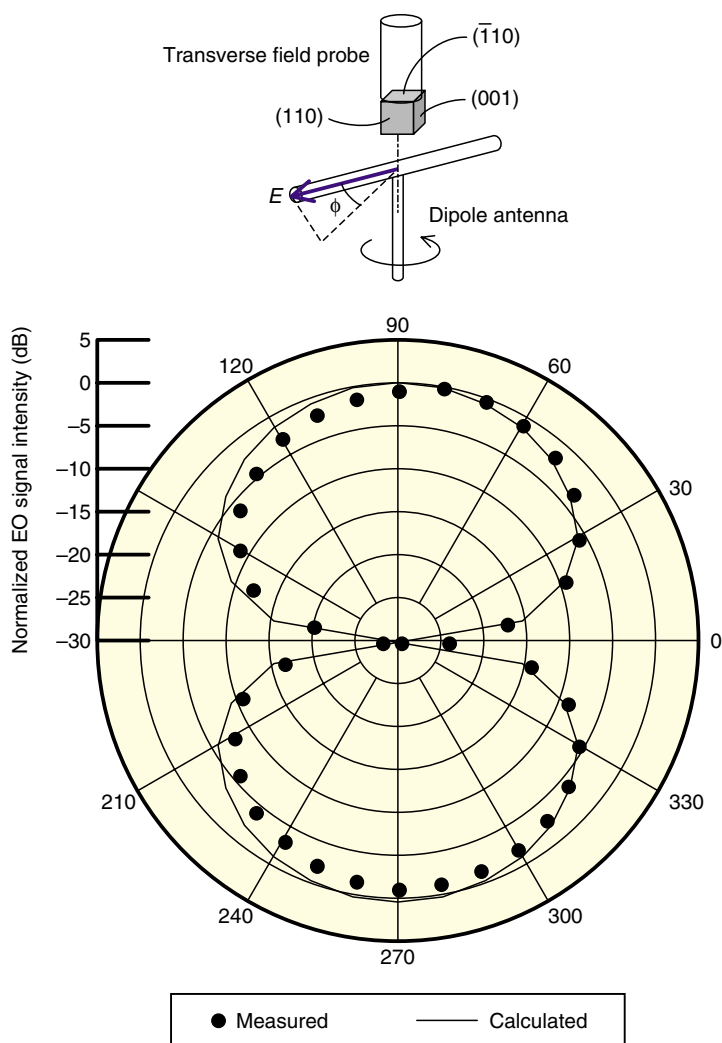Fig. 8. Directivity of longitudinal field probe.
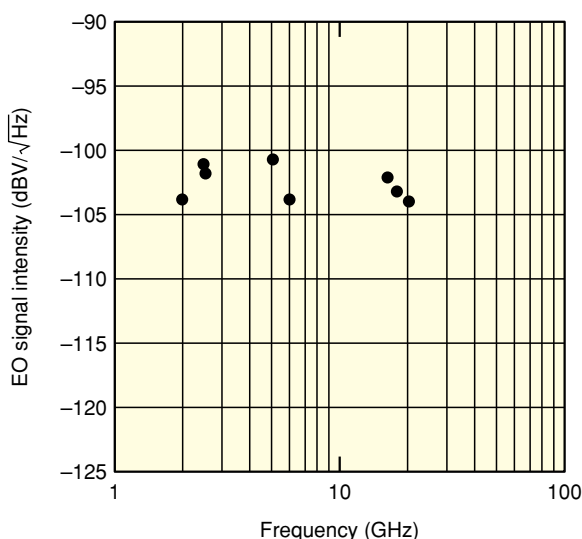
Fig. 9. Directivity of transverse field probe.

Fig. 10. Frequency characteristics.

represents the calculated [001]-direction component of the applied electric field at each rotation angle θ. All values were normalized by their maximum values. For both planes, the measured intensities agreed with the calculated ones and the cross-axis isolation ratio was over 45 dB. In Fig. 9, closed circles show the directivity of the measured electric field intensity and the solid line shows that of the intensities calculated to be projected in the [110] direction at angle ϕ of dipole antenna rotation from the [1$\bar{1}$0] direction. These values were also normalized by the maximum values. The measured intensities agreed with the calculated ones and the cross-axis isolation ratio was over 35 dB, which is large enough to isolate the sensitivity from the null direction. These results demonstrate that it is possible to measure an electric field vector by aligning the EO probes orthogonally.

3.4 Frequency response

The relationship between the frequency of the applied electric field and the EO signal intensity obtained for the transversal field probe is shown in **Fig. 10**. In this measurement, electric fields were applied to the EO probe at frequencies ranging from 1.95 to 6 GHz and from 16 to 20 GHz using a half-wavelength dipole antenna and a rectangular horn antenna, respectively. The electric field at the EO probe tip was always set to 34 V/m by calibrating the input power to the antennas with a commercially available electric field sensor (NARDA EMC300). The results indicate that the uniformity of the sensitivity was better than ±2 dB in the range from 1.95 to 20 GHz.

4. Electric field measurement

4.1 Near-field measurement around a dipole antenna

We measured the near field around a 2.45-GHz-band dipole antenna using the longitudinal field probe in the shielded box. The probe was scanned parallel to the radial axis of the dipole antenna while a sinusoidal signal from a signal generator was input to the antenna. The relationship between distance from the dipole antenna and EO signal intensity is shown in **Fig. 11**. Closed circles and the solid line represent measured and calculated intensities nor-
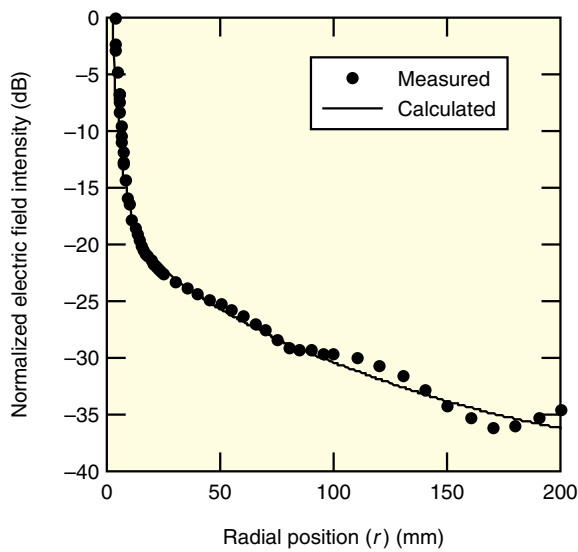
Fig. 11. Near-field distribution around dipole antenna in free space.

malized by their maximum values. In the near-field region where electrostatic coupling and inductive electromagnetic coupling are dominant, the measured intensities agreed with the calculated ones very well. This demonstrates that the EO probe can accurately measure a near field around the dipole antenna. In the region more than 100 mm away from the dipole antenna, some differences between the measured and calculated intensities were observed because the composition of the shielded box was not included in the calculation. The measured intensities represent a standing wave caused by reflection from the box walls.

4.2 Electric field measurement in tissue-equivalent phantom

We measured the specific absorption rate (SAR) as an example of electric field measurements that can be performed using this EO probe. SAR is the primary dosimetric parameter of RF energy absorbed by the human body and is determined from the electric field distribution in the human body [7]-[9]. Because the SAR of mobile phones must be less than the lower limit stipulated in the regulations [7]-[9], measuring the electric field distribution in a TEP is very important in mobile phone development.

The setup for the electric field measurement in the TEP is shown in **Fig. 12** [10]. A rectangular acrylic case was filled with the TEP and a 2.45-GHz-band dipole antenna was positioned 5 mm below the case. We scanned the transverse field probe parallel and
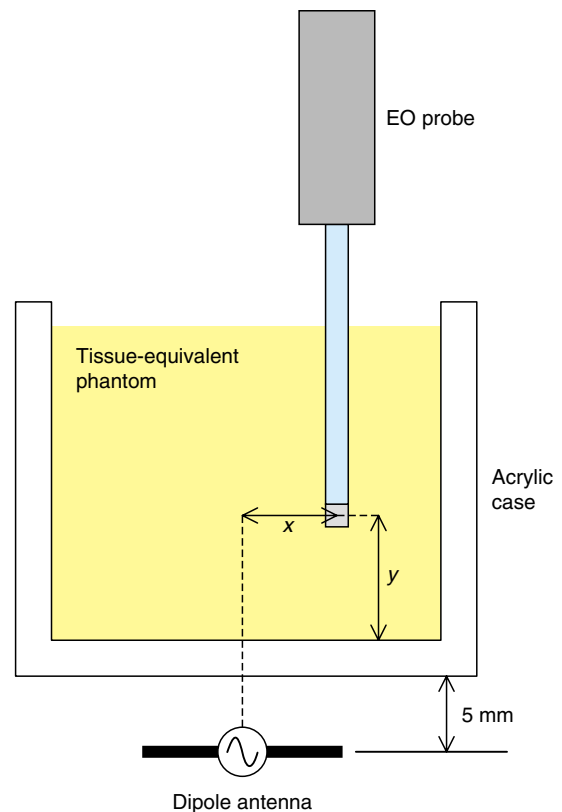

Fig. 12. Electric field measurement system in tissue-equivalent phantom.

perpendicular to the base of the case while an RF signal with power of 17 dBm was fed into the dipole antenna. The intensity and phase of the electric field were obtained using the equivalent sampling method [11]. Electric field distributions parallel and perpendicular to the base are shown in **Fig. 13**. Closed and open circles represent the EO signal intensities and phases. The minimum distance from the base was 1 mm, which is less than one fifth the distance used for a conventional probe. In a previous experiment using an electric field probe reported by another group, there were differences between the simulated and measured values near the base because of electrical coupling between the probe and base [12]. In this work, on the other hand, we obtained correct data even when the EO probe was set within 1 mm of the base (Fig. 13(b)). The minimum detectable electric field was less than 0.6 V/m, corresponding to an SAR that satisfies the minimum detection limit [7]-[9]. These results demonstrate the applicability of the EO probe to SAR measurement.

● Intensity   ○ Phase
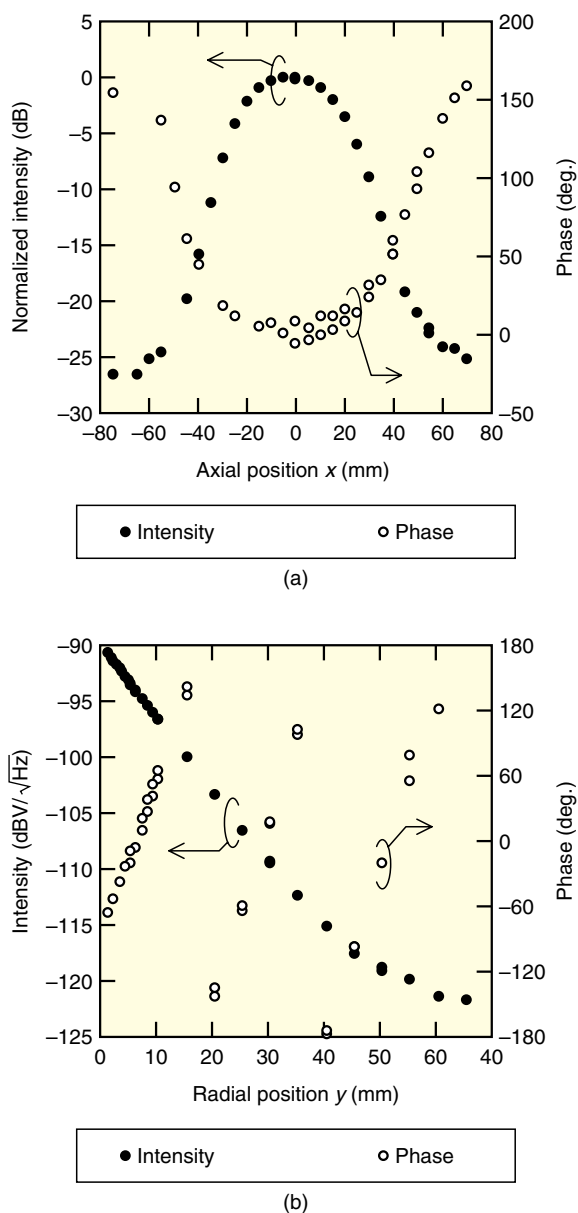
(a)

● Intensity   ○ Phase

(b)

Fig. 13. Electric field distribution in tissue-equivalent
phantom parallel (a) and perpendicular (b) to
the antenna axis.

5. Conclusions

We have developed a tip-on-fiber EO probe for
near-field measurement. This probe contains no
metallic components and the EO crystal is fixed on
the tip of an optical fiber that connects the crystal to
the optical components to eliminate disturbances,
such as optical and electrical components, from the
near-field range. As a result, electric field measure-
ments can be performed with little invasiveness. We

developed longitudinal and transverse field probes
that detect electric fields orthogonal to each other.
The near-field measurement system has a dynamic
range of over 45 dB and can detect an electric field of
less than 0.6 V/m. The EO probe has excellent direc-
tivity with a cross-axis isolation ratio of over 45 dB.
A comparison between the measured and calculated
near fields around the dipole antenna confirmed that
the probe's invasiveness is negligible. An electric
field measurement using a tissue-equivalent phantom
demonstrated the applicability of this measurement
system to specific absorption rate.

References

[1] E. B. Joy, W. M. Leach, G. P. Rodrigue, and D. T. Paris, "Applica-
tions of probe-compensated near-field measurements," IEEE Trans.
Antennas Propag., Vol. 26, No. 3, pp. 379-389, May 1978.
[2] H. I. Bassen and G. S. Smith, "Electric field probes—A review,"
IEEE Trans. Antennas and Propag. Vol. 31, No. 5, pp. 710-718, Sep.
1983.
[3] K. Pokovic, "Advanced electromagnetic probes for near-field evalua-
tions," Dissertation of Swiss Federal Institute of Tech., Zurich,
Switzerland, 1999.
[4] N. Kuwabara, K. Tajima, R. Kobayashi, and F. Amemiya, "Develop-
ment and analysis of electric field sensor using $LiNbO_3$ optical mod-
ulator," IEEE Trans. Electromagnetic Compatibility, Vol. 34, No. 4,
pp. 391-396, Nov. 1992.
[5] B. G. Loader, M. J. Alexander, W. Liang, and S. Torihata, "An Opti-
cal Electric Field Probe for Specific Absorption Rate Measurements,"
15th International Zurich Symposium on Electromagnetic Compati-
bility, 12C3, pp. 57-60, Zurich, Switzerland, 2003.
[6] H. Togo, A. Sasaki, A. Hirata, and T. Nagatsuma, "Characterization
of millimeter-wave antenna using photonic measurement tech-
niques," Int. J. RF and Microwave CAS, Vol. 14, pp. 290-297, 2004.
[7] ICNIRP, "Guidelines for limiting exposure to time-varying electric,
magnetic, and electromagnetic fields (up to 300 GHz)," Health
Physics, Vol. 74, No. 4, pp. 494-522, Apr. 1998.
[8] "IEEE standard for safety levels with respect to human exposure to
radio frequency electromagnetic fields, 3 kHz to 300 GHz,"
ANSI/IEEE Standard C95.1-1991, Apr. 1992.
[9] "Radio-radiation protection guidelines for human exposure to elec-
tromagnetic fields," Telecommunication Technology Council, Min-
istry of Posts and Telecommunication, Deliberation Rep. 89, Tokyo,
Japan, 1997 (in Japanese).
[10] T. Onishi, H. Togo, N. Shimizu, K. Kiminami, S. Uebayashi, and T.
Nagatsuma, "SAR measurement employing electro-optic (EO) probe
without using metal," in a joint meeting BioEM2005, Dublin, Ireland,
June 2005.
[11] A. Sasaki and T. Nagatsuma, "Millimeter-wave imaging using an
electrooptic detector as a harmonic mixer," IEEE Q. Electron., Vol. 6.
No. 5, pp. 735-740, Sep. 2000.
[12] T. Schmid, O. Egger, and N. Kuster, "Automated E-field scanning
system for dosimetric assessments," IEEE Trans. Microwave Theory
Technol., Vol. 44, No. 1, pp. 105-113, Jan. 1996.

Hiroyoshi Togo

Research Engineer, Smart Devices Laboratory, NTT Microsystem integration Laboratories.

He received the B.S. degree in electronic engineering from Meiji University, Kanagawa in 1994 and the M.S. degree in applied physics from the University of Tsukuba, Ibaraki in 1996. He joined NTT Musashino Opto-electronics Laboratories in 1996. From 1996 to 2001, he was engaged in the development of the thermo-capillary optical switch (OLIVE switch) and from 2001 to 2002 he endeavored to commercialize it for NTT Electronics Inc. Since 2002, he has been researching ultrawideband impulse radio (UWB-IR) systems using photonic techniques at NTT Microsystem Integration Laboratories, Kanagawa. He is a member of the Institute of Electronics, Information and Communication Engineers (IEICE) of Japan and the Japan Society of Applied Physics (JSAP).

Tadao Nagatsuma

Group Leader, Microwave and Photonics Systems Research Group, Smart Devices Laboratory, NTT Microsystem integration Laboratories.

He received the B.S., M.S., and Ph.D. degrees in electronic engineering from Kyushu University, Fukuoka in 1981, 1983, and 1986, respectively. He joined NTT Atsugi Electrical Communications Laboratories, Kanagawa in 1986. His current research involves ultrahigh-speed electronics and millimeter-wave photonics and their application to sensors and communications. He is a senior member of IEEE and a member of the Optical Society of America. He received the 1989 Young Engineers Award from IEICE, the 1992 IEEE Andrew R. Chi Best Paper Award, the 1997 Okochi Memorial Award, the 1998 Japan Microwave Prize, the 2000 Minister's Award of the Science and Technology Agency, and the 2002 Asia Pacific Microwave Conference APMC Prize.

Naofumi Shimizu

Senior Research Engineer, Smart Devices Laboratory, NTT Microsystem integration Laboratories.

He received the B.E., M.E., and D.E. degrees in engineering physics from Kyoto University, Kyoto in 1986, 1988, and 2004, respectively. He joined NTT LSI Laboratories, Kanagawa in 1988 and engaged in R&D of III-V high-speed devices. Since 1998, he has been with NTT Lightwave Communications Laboratory, where he has been engaged in research on high-speed lightwave transport systems. He is currently engaged in R&D of millimeter-wave photonic devices and systems. He is a member of IEICE, JSAP, and IEEE. He was a recipient of the 2001 IEICE Electronics Society Prize.